Article

Study of 13Cr-4Ni-(Mo) (F6NM) Steel Grade Heat Treatment for Maximum Hardness Control in Industrial Heats

Massimo De Sanctis [1,*], Gianfranco Lovicu [2], Massimiliano Buccioni [2], Angelo Donato [2], Maria Richetta [3] and Alessandra Varone [3]

[1] Dipartimento di Ingegneria Civile e Industriale, Università di Pisa, Largo Lucio Lazzarino, 2, 56122 Pisa, Italy

[2] Nuovo Pignone Tecnologie Srl, BHGE, Via Felice Matteucci, 2, 50127 Firenze, Italy; gianfranco.lovicu@bhge.com (G.L.); Massimiliano.Buccioni@bhge.com (M.B.); Angelo.Donato@bhge.com (A.D.)

[3] Dipartimento di Ingegneria Industriale, Università di Tor Vergata, Via del Politecnico, 1, 00133 Roma, Italy; richetta@uniroma2.it (M.R.); alessandra.varone@uniroma2.it (A.V.)

* Correspondence: m.desanctis@ing.unipi.it; Tel.: +39-050-2217827

Abstract: The standard NACE MR0175 (ISO 15156) requires a maximum hardness value of 23 HRC for 13Cr-4Ni-(Mo) steel grade for sour service, requiring a double tempering heat treatment at temperature in the range 648–691 °C for the first tempering and 593–621 °C for the second tempering. Difficulties in limiting alloy hardness after the tempering of forged mechanical components (F6NM) are often faced. Variables affecting the thermal behavior of 13Cr-4Ni-(Mo) during single and double tempering treatments have been studied by means of transmission electron microscopy (TEM) observations, X-ray diffraction measurements, dilatometry, and thermo-mechanical simulations. It has been found that relatively low Ac_1 temperatures in this alloy induce the formation of austenite phase above 600 °C during tempering, and that the formed, reverted austenite tends to be unstable upon cooling, thus contributing to the increase of final hardness via transformation to virgin martensite. Therefore, it is necessary to increase the Ac_1 temperature as much as possible to allow the tempering of martensite at the temperature range required by NACE without the detrimental formation of virgin martensite upon final cooling. Attempts to do so have been carried out by reducing both carbon (<0.02% C) and nitrogen (<100 ppm) levels. Results obtained herein show final hardness below NACE limits without an unacceptable loss of mechanical strength.

Keywords: supermartensitic stainless steels; tempering treatments; austenite reversion

1. Introduction

Low-carbon supermartensitic stainless steel 13Cr-4Ni-(Mo) has substituted 12% Cr for several decades, and more recently, CA15 steels in many applications in the oil/gas industry [1,2]. The combination of low carbon content with the addition of 3.5–4.5% Ni suppresses the formation of δ-ferrite and promotes the formation of a mixed structure of α′ (martensite) and γ (austenite) at room temperature, which possesses superior mechanical properties and corrosion resistances [3–5]. This alloy is proposed in two delivery conditions: casted (CA6NM) or forged (F6NM), and it finds wide applications for handling fluids containing CO_2 and H_2S. These environments increase the danger of sulfide stress corrosion cracking (SSCC); the NACE MR0175 standard limits 13Cr-4Ni alloys to 23 HRC maximum for sour service. However, in industrial practice, considerable difficulties are faced in lowering the hardness of 13Cr-4Ni-(Mo) below 23 HRC. These difficulties are of crucial interest, since tempering

treatments are carried out on expensive mechanical components (e.g., compressor rotors) in their final state. Tempering should maximize the recovery of the martensitic matrix and promote the retention of soft retained austenite at room temperature. Previous studies on the thermal behavior of low-carbon 13Cr-4Ni alloy [2] and 16Cr-5Ni-(Mo) [6] showed that the amount of retained austenite increases with increasing reversion treatment temperature, exhibiting a peak typically in the range 620–640 °C. Above this range, it decreases with increasing temperatures, leading to the formation of virgin martensite upon cooling, with increasing hardness. It has been suggested that the stability of reversed austenite initially increases because of the diffusion of nickel and other gamma-stabilizing elements from the martensitic matrix towards reverted austenite islands [7–9]. Above a critical tempering temperature, a gradual loss of stability would occur because of several factors, among which the most important seems to be the solute redistribution for increasing volume fractions of reversed austenite [10]. The NACE MR0175 standard requires a double tempering treatment after quenching for F6NM, with a tempering temperature within 650–690 °C for the first tempering and 595–620 °C for the second one. An initial high-temperature treatment which is even higher than the Ac_1 temperature of the alloy will favor softening of as-quenched martensite, and at the same time, the formation of reverted austenite, which can at least partially transform into virgin martensite upon cooling. The aim of the second stage of tempering is the recovery of the newly formed virgin martensite. Experimental diagrams are available for 13Cr4Ni0.5Mo [11], giving the final hardness and content of retained austenite at room temperature as a function of temperature and time of tempering treatments using a "Larson–Miller"-type parameter $(P = T(\mathrm{K})[20 + \log t(\mathrm{h})] \times 10^{-3})$. For 13Cr4Ni0.5Mo after single heat treatment, most reverted austenite formed up to $P = 17.7$ is expected to remain stable while cooling to room temperature, and according to these data sets, hardness would attain a minimum of 250 HB. Double treatments are indicated as effective in reducing hardness around 220 HB—at least when the second tempering is carried out below $P = 18.2$. Nevertheless, from industrial experience and previous indications, there is a considerable scatter of results with related economic losses.

Gooch [12] studied the effects of heat treatments for welded 13Cr4Ni steels, and agreed on the difficulty in limiting the alloy hardness through post-weld heat treatments. He concluded that the major compositional factor determining hardness was carbon, which should be limited below 0.03%. The objective of this work is to carry out a detailed study on microstructural transformations occurring during single and double temper treatments of 13Cr4Ni(Mo) steel, with the aim of clarifying the compositional and microstructural variables influencing the final hardness of this alloy and to give useful guidelines for industrial practice.

2. Materials and Methods

Two industrial heats of 13Cr4Ni0.5Mo have been considered in this work, with chemical compositions reported in Table 1.

Table 1. Chemical composition of the studied alloys.

Heats	%C	%Si	%Mn	%P	%Cr	%Mo	%S	%Ni	N (ppm)	%Cr$_{eq}$/%Ni$_{eq}$ *
A	0.027	0.35	0.90	0.019	12.89	0.52	0.001	3.84	180	2.45
B	0.030	0.44	0.73	0.018	12.72	0.55	0.001	3.85	280	2.35

* %Ni$_{eq}$ and %Cr$_{eq}$ calculated following the DeLong formula.

The compositions are very close, with an almost coincidental Cr$_{eq}$/Ni$_{eq}$ ratio. The only significant differences are the higher carbon (0.03% C) and nitrogen (280 ppm) contents in Heat B than in Heat A (0.027% C, 180 ppm N).

These industrial heats were processed through the following treatments:

- Homogenizing at 1473 K (1200 °C) for 4 h, followed by preliminary hot forging (HR);
- Intermediate stress relief at 700 °C;

-     Forging (F samples) at 1473 K (1200 °C);
-     Austenitizing 4 h at 1020 °C followed by oil quenching (OQ) to room temperature.

The Ac_1 and Ms critical temperatures were determined by dilatometric analysis using a Gleeble 3800 thermo-mechanical simulator (Dynamic Systems Inc., Poestenkill, NY, USA), equipped with a ISO-Q Quenching and Deformation Dilatometer. The samples were heated at 1020 °C, with a heating rate of 300 °C/h, held for 1 h at the target temperature, and then cooled to room temperature using different cooling rates of 100 and 3000 °C/h. Volume variations of samples were measured by a laser dilatometry system [13]. Figure 1 shows the geometry and dimensions of the samples used. Details of the experimental technique are reported elsewhere [14].
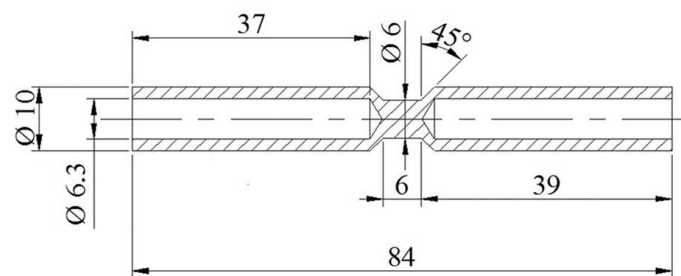
Figure 1. Geometry of the sample used for dilatometric analysis (unit: mm).

The Gleeble® 3800 simulator has also been used to reproduce single and double tempering treatments in the temperature range 610–700 °C using heating rates of 300 °C/h with holding times of 1 h followed by air cooling. Treated samples have been used to determine their mechanical properties. The volume fraction of retained austenite at room temperature (γ_r) was determined by X-ray diffraction (Philips, Eindhoven, The Netherlands). XRD spectra were collected in the 2θ angular range 5° to 65° by using the Mo-Kα radiation ($\lambda = 0.71$ Å) in step scanning mode with steps of 0.05° and counting time of 5 s per step. The relative amounts of martensite and retained austenite were calculated for each sample from the integrated intensities of the reflections of both phases, following the ASTM E975 standard [15].

Mechanical properties were measured by means of tensile tests on a Galdabini® SUN 1000 tensile machine (Cardano al Campo (VA), Italy). Tensile specimens which were 1 mm in thickness, 12.5 mm in width, and with a gage length of 50 mm, heat treated by Gleeble 3800 as described above have been used. Tests were performed using a crosshead displacement rate of 1 mm/s, and the gage length elongation was measured using an extensometer. To compare the quantity of austenite in the microstructure of samples subjected to different quenching and tempering treatments, the instantaneous strain-hardening coefficient (n) was evaluated. It is defined as follows:

$$n = \frac{d(\ln \sigma)}{d(\ln \varepsilon)} \tag{1}$$

where σ and ε are true stress and true strain, respectively.

The presence of the austenitic phase—with its associated high work hardening behavior—induces high n values and pronounced plateau in the n vs. true strain curves, depending on its volume fraction and stability. Moreover, it is also responsible for the observed marked serration in the instantaneous strain hardening curves [16].

Microstructural studies have been carried out by transmission electron microscopy (TEM) using a Philips® CM12 microscope (Philips Electron Optics, Eindhoven, The Netherlands) equipped with a Bruker® Quantax TEM 200T EDX system (Bruker, Berlin, Germany). Thin foils were prepared by mechanical grinding followed by double-jet electropolishing in a solution of 10% perchloric acid and 90% butoxyethanol at 258 K (-15 °C) and 9 V.

Alloy hardness was measured using Rockwell (Hardness tester, C.I.S.A.M. sas, Induno Olona, Italy) tests from industrial byproducts and Vickers (Micro-hardness tester, Shimadzu Corporation, Kyoto, Japan) tests from 1 mm-thick heat-treated samples used in the Gleeble 3800 simulator. The Vickers hardness scale is frequently used for these heats for weld procedure qualification tests, and according to the BS860 1967 standard, a 23 HRC limit would be equivalent to 253 HV. It has been shown that this conversion—as well as the ASTM E140-88 correlation—is not applicable to 13Cr-4Ni-(Mo) materials, with several researchers indicating 23 HRC as equivalent to 275 HV [17,18]. Therefore, this hardness equivalence will be used hereinafter.

3. Results

Table 2 compares the hardness values of preliminary hot forged (HR) and as-quenched (after forging) (OQ) samples from different heats. In spite of their similar chemical compositions, hot rolled samples are very different in hardness, with Heat A (31.1 ± 1.0 HRC) being significantly harder than Heat B (25.1 ± 0.8 HRC).

Table 2. Hardness of Heats A and B in hot rolled (HR) and oil quenched (OQ) conditions.

Heat	Hardness (HRC)	
	HR-Samples	**As-Quenched Samples**
A	31.1 ± 1.0	35.3 ± 1.3
B	25.1 ± 0.8	34.2 ± 1.2

The hardness difference was partially recovered in OQ samples where Heat B (34.2 ± 1.2 HRC) showed about the same hardness as Heat A (35.3 ± 1.3 HRC). Considering that the hardness value is also affected by the amount of retained austenite, the Ms–Mf range for Heat A is expected to be higher in temperature than for Heat B.

The Ms and Ac_1 critical temperatures have been determined through dilatometric analysis, and relevant experimental curves for Heat A and Heat B are reported in Figure 2.

The experimental Ac_1 temperatures for Heats A and B were calculated from the dilatometric curves and by analyzing their derivatives. Figure 3 shows the derivative curves in the range of temperature close to the transformation point. Three different curves have been considered, performed at different cooling rates (two samples at 100 °C/h and one at 3000 °C/h), but with the same heating rate (300 °C/h). For the same Heat, there is a good agreement among the Ac_1 temperatures determined from different samples. The uncertainty of calculated Ac_1 was determined using the temperature range in which it is possible to verify the slope change of dilatometric curves and their derivatives.
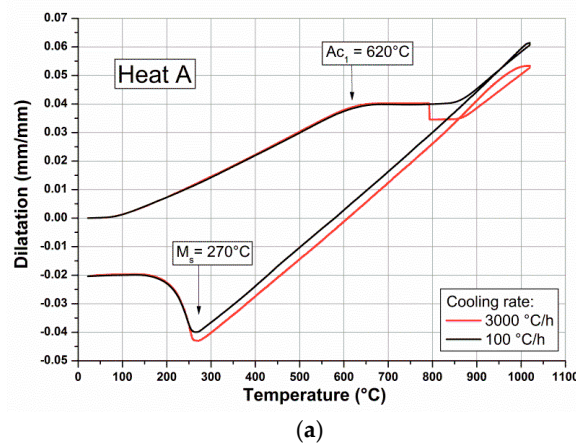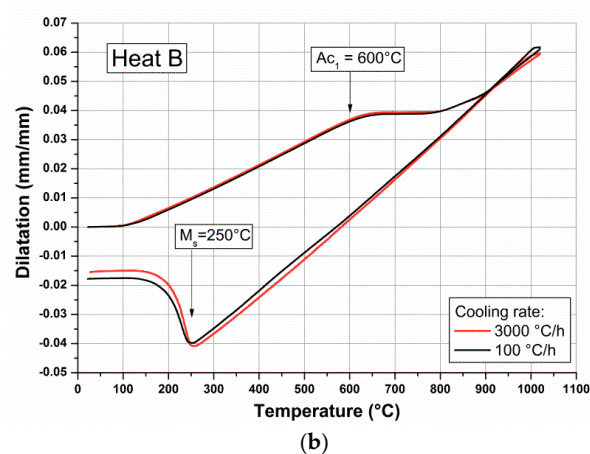

(a)

Figure 2. *Cont.*

(**b**)

Figure 2. Dilatometric curves of (**a**) Heat A and (**b**) Heat B.
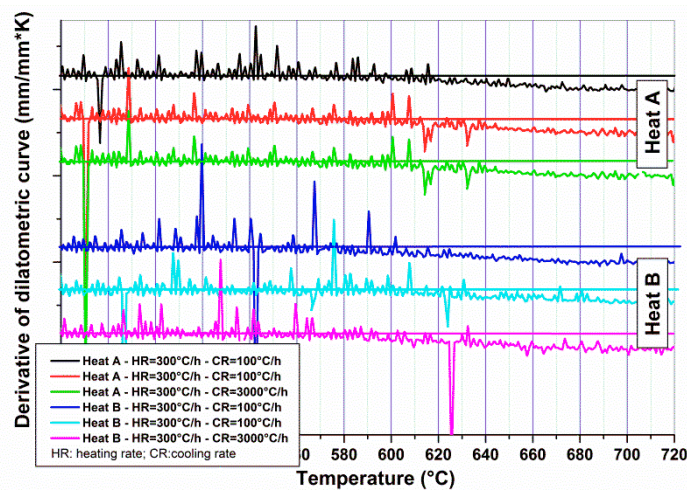

Figure 3. Derivatives of dilatometric curves of Heat A and Heat B samples. Different curves have been shifted to avoid overlapping and to allow a better comparison among them.

Ac_1 temperatures for Heat A and B were around 620 ± 10 and 600 ± 10 °C, respectively. These results could be compared to the calculated Ac_1 temperature for 13% Cr steels having carbon contents lower than 0.05% [19], according to the following formula:

$$Ac_1(°C) = 850 - 1500(C + N) - 50Ni - 25Mn + 25Si + 25Mo + 20(Cr - 10) \tag{2}$$

The predicted Ac_1 temperature for Heats A and B were 647 and 633 °C, respectively. These values are higher than the experimental temperature, although it is confirmed that the Ac_1 temperature of Heat A is higher with respect to Heat B.

The Ms temperature for Heat B (250 ± 10 °C) is lower than Heat A (270 ± 15 °C), thus supporting the propensity for this alloy to retain higher volume fractions of austenite in HR and OQ products.

Figure 4 shows electron micrographs from OQ samples of Heat A and Heat B. The microstructures consist of an α' martensite matrix, in which fine and highly dislocated laths are distributed parallel to one another. The presence of retained austenite is not evident in OQ state, being scarcely visible only in Heat B in the form of thin interlath films (Figure 4b).

Figure 5 shows stress–strain curves and Figure 6 yield strength (YS) and ultimate tensile strength (UTS) values obtained on OQ samples heat treated (tempered) by Gleeble 3800 for one hour at different temperatures in the temperature range 610–700 °C.
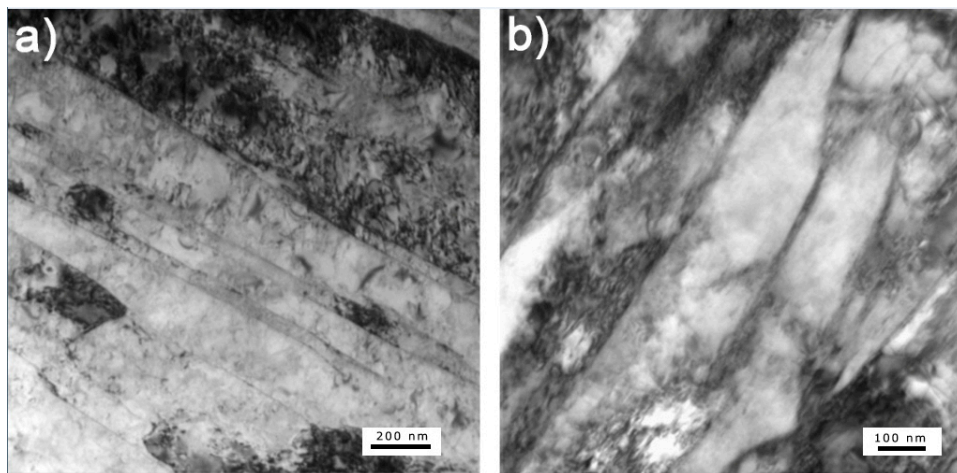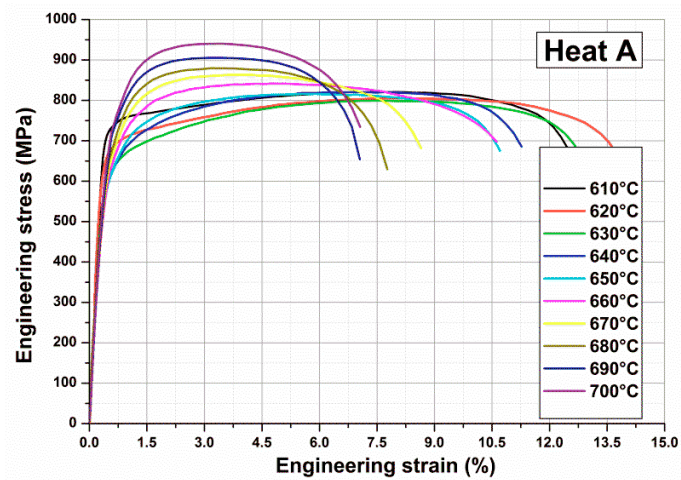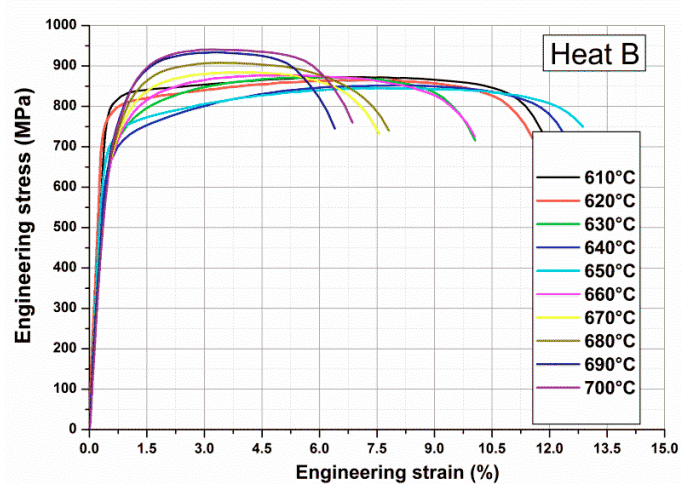
Figure 4. TEM electron micrographs of (**a**) Heat A and (**b**) Heat B after oil quenching (OQ samples).

(**a**)

(**b**)

Figure 5. Experimental stress–strain curves of (**a**) Heat A and (**b**) Heat B after single tempering at different temperatures.
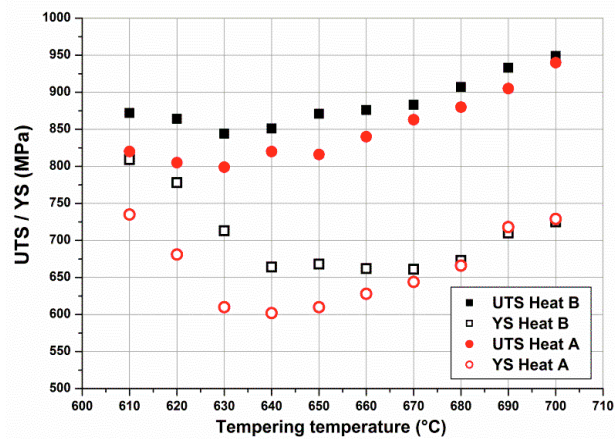
Figure 6. Yield (YS) and tensile (ultimate tensile strength, UTS) strengths of Heat A (red) and Heat B (black) after single tempering at different temperatures (610–700 °C).

The Vickers hardness (HV10) measurements of these samples are shown in Figure 7. It can be observed that Heat B remained constantly harder than the limit of 275 HV (23 HRC), whereas the hardness reduction of Heat A allowed values close to the limit. Moreover, for both heats there was a slight decrease of strengths and hardness when increasing the tempering temperature from 610 to around 650 °C, followed by a step increase for higher temperatures.

Figure 8 shows volume fractions of retained austenite measured in Heat A and Heat B after single tempering. The austenite content of both heats was relatively low, with the values consistently below 10%. For Heat B the peak was reached at 630 °C, whereas for Heat A it was around 640 °C.

Strength and hardness were reduced in the presence of retained austenite, but they showed a further increase when austenite disappeared, as shown in Figure 6. This was also confirmed by the instantaneous strain hardening coefficient, n, measured during tensile tests of single tempered samples, as shown in Figure 9. This coefficient is sensitive to all factors influencing the strain hardening behavior of the steel. For steels whose microstructure is a mixture of martensite and austenite, both the mean value and the punctual variability of n were affected by relative amounts of soft retained austenite. As shown in Figure 9, the gradual loss of stability of reverted austenite for tempering temperatures above 640 °C in Heat A is apparent, with a practical absence of retained austenite at room temperature for tempering treatments above 670 °C.
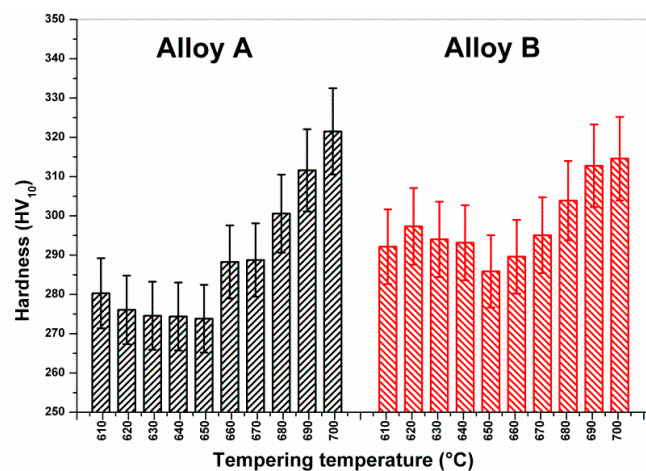

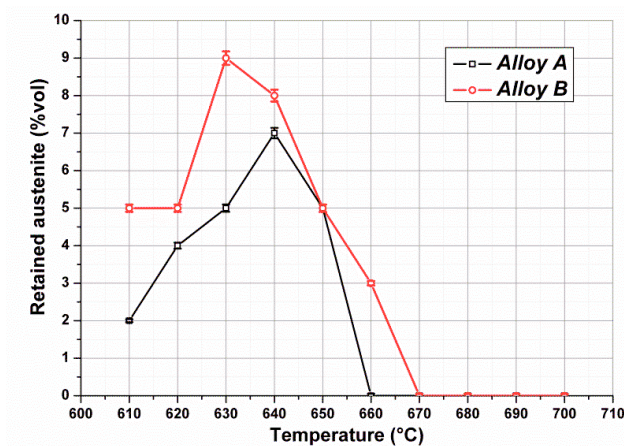**Figure 7.** Hardness values for Heat A and Heat B as a function of the single tempering treatment.

Figure 8. Volume fraction of retained austenite in function of tempering temperatures.
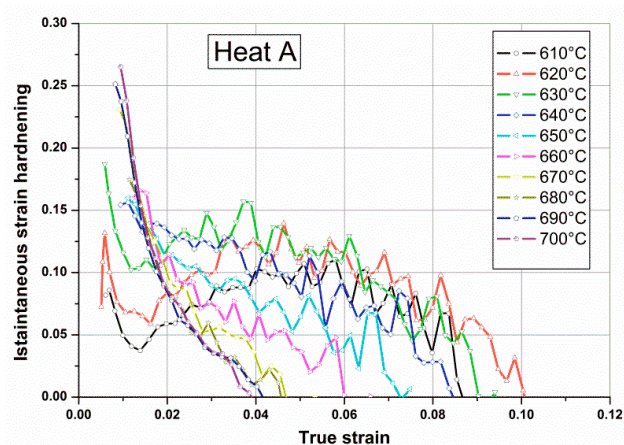

Figure 9. Instantaneous strain hardening coefficient of Heat A after different tempering treatments.

From these results, the final hardness after single tempering appears to be the result of both the structural recovery of untempered martensite and the relative stability of reverted austenite during previous heating. Strength and hardness initially decreased after single tempering above 600 °C due to increased recovery of as-quenched martensite and the retention of stable retained austenite. For increasing temperatures, reverted austenite became unstable, forming virgin martensite upon cooling, thus determining a further increase of both hardness and strength.

Figure 10 shows the microstructure of Heat A after single tempering at 620 °C (Figure 10a) and 680 °C (Figure 10b), respectively, below and above the critical temperature for austenite destabilization upon cooling. The microstructure of samples tempered at 620 °C consisted of tempered martensite with elongated islands of retained austenite formed in the interlath regions with no evidence of untempered martensite. After tempering at 680 °C, many islands of highly dislocated virgin martensite were observed.

Finally, Figure 11 shows the alloy microstructure after tempering at 650 °C, where all possible structural constituents may coexist—specifically, recovered original martensite, virgin martensite, and retained stable austenite.

As shown in Figure 11 and Table 3, image contrast coupled with energy-dispersive X-ray spectroscopy (EDS) measurements can be conveniently used to distinguish between different constituents. Regions where α' to γ reversion occurred are characterized by an increased amount of both Ni and Mn compared to the nominal heat composition, as a consequence of solute redistribution between phase constituents during tempering.
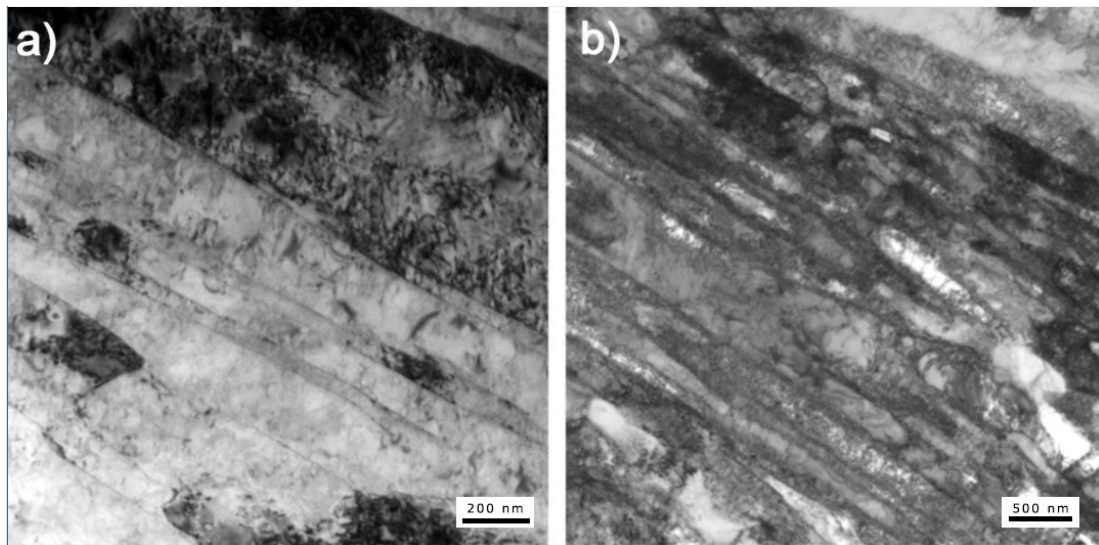
Figure 10. TEM electron micrographs of Heat A after single tempering treatment at: (**a**) 620 °C and (**b**) 680 °C.
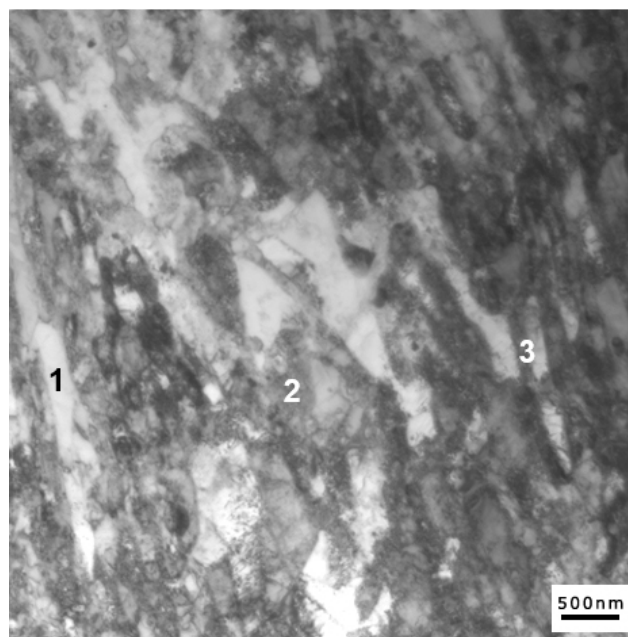

Figure 11. TEM micrograph of Heat A tempered at 650 °C. Numbers in the figure identify the regions where Energy dispersive X-ray EDX microanalysis was performed. Results for Cr, Mn, and Ni weight percentages are reported in Table 3.

Table 3. Content of Cr, Mn, and Ni measured by EDX microanalysis from the different regions marked in Figure 11.

Region Marked in Figure 11	wt % Cr	wt % Mn	wt % Ni
1 (retained austenite)	12.47 ± 0.5	2.40 ± 0.2	7.32 ± 0.3
2 (tempered martensite)	13.57 ± 0.4	0.76 ± 0.1	3.30 ± 0.2
3 (virgin martensite)	13.16 ± 0.7	1.99 ± 0.3	5.07 ± 0.2

Among these areas, retained austenite islands can be further distinguished by a low density of dislocations (Figure 11, Region 1), in contrast to virgin martensite with a high density of dislocations (Figure 11, Region 3). Finally, regions of tempered martensite are characterized by decreased nickel content compared to the nominal heat composition, as well as by partial recovery of the martensitic matrix (Figure 11, Region 2).

The effect of a second tempering treatment was investigated, taking into consideration NACE recommendations for the first cycle (for which NACE requires a temperature in the range 648–690 °C); two temperatures corresponding to the presence or total absence of stable austenite were chosen: 650 °C (P = 18.4) and 680 °C (P = 19.0), respectively. For the second cycle, the minimum and maximum NACE-recommended temperatures—595 °C (P = 17.3) and 620 °C (P = 17.9)—were used. Figure 12 shows YS and UTS, and Figure 13 shows the hardness after double tempering.
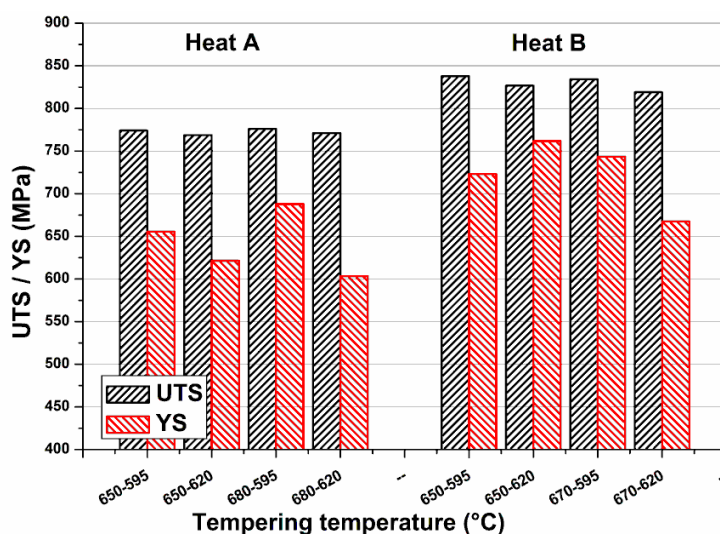

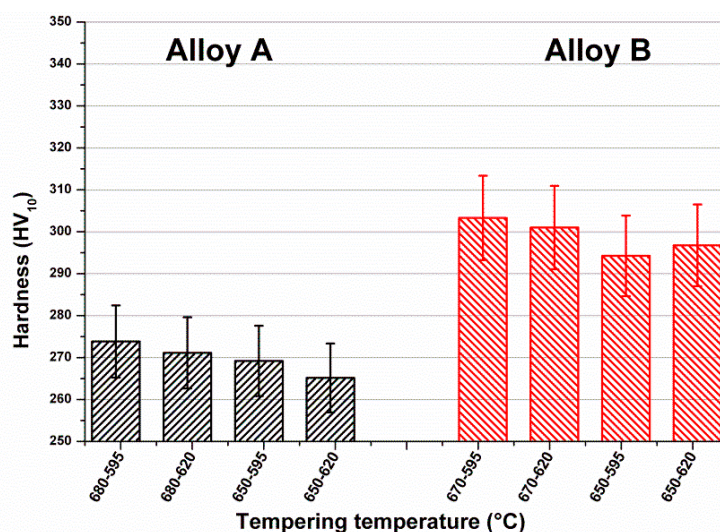**Figure 12.** YS and UTS of Heat A and Heat B following double temper treatments.

Figure 13. Hardness values for Heat A and Heat B in function of double tempering treatments.

Both tensile strength and hardness levels were significantly lower compared to the first tempering cycle, with hardness reduced to 266 HV after 1 h at 650 °C, and 1 h at 620 °C, whereas no useful reductions were obtained for Heat B, with tensile strengths above 800 MPa, with hardness values remaining around 300 HV10.

The effects of intermediate and final sub-zero cooling ($-30\ °C$) for double tempering treatment were studied using $650\ °C$ for the first tempering temperature and varying the temperature of the second cycle from 595 to $620\ °C$. The results reported in Figure 13 indicate that an intermediate cooling between the first and the second temper was beneficial for the reduction of hardness, especially for Heat B, thus confirming Gooch's suggestions [12].

Moreover, a final sub-zero treatment—which is expected to partially destabilize retained austenite—induced an increase in hardness, especially for Heat B (as shown in Figure 14).
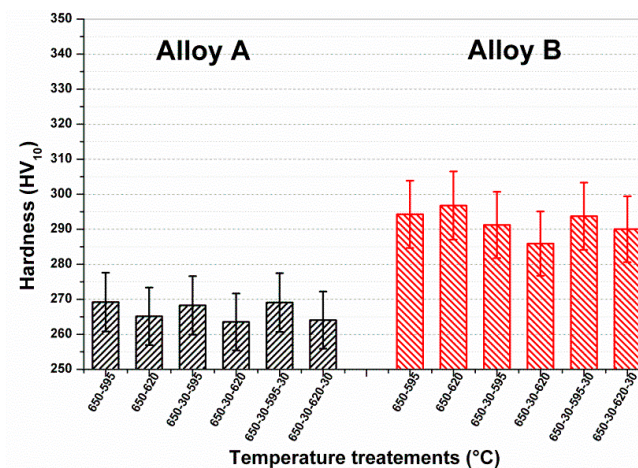

Figure 14. Hardness values for Heat A and Heat B following double tempering treatments with intermediate and final sub-zero ($-30\ °C$) cooling.

4. Discussion

Despite similar chemical compositions and almost similar Cr_{eq}/Ni_{eq} ratios of Heats A and B, their responses to heat treatments were rather different. It is apparent that a significant reduction of hardness below the NACE limit (23 HRC) could be accomplished only for Heat A, whereas Heat B remained hard while also adopting the double tempering strategy recommended by NACE standards.

In order to obtain significant hardness reductions after tempering, the as-quenched martensite matrix should recover at high temperatures, allowing the retention of soft austenite islands without destabilization to virgin martensite. For the industrial heats studied, two major difficulties are presented. The first difficulty is to obtain significant volume fractions of stable retained austenite at room temperature, potentially as a result of the relatively high Ms values measured (Figure 2). The second difficulty is an intrinsic instability of reversed austenite formed at a temperature that favors the transformation to virgin martensite during cooling and limits the hardness reduction after tempering in the final product.

The stability of reversed austenite decreased during tempering as consequence of solute partitioning of γ-stabilizer elements (especially Ni and C). As the tempering temperature increases, the volume fraction of reversed austenite increases and the consequent solute redistribution is no longer able to stabilize the γ phase on cooling. This aspect is believed to be critical for 13Cr-4Ni-(Mo) industrial heats, which are characterized by relatively low carbon and nickel contents as compared to other supermartensitic alloys [6]. Moreover, alloying with molybdenum (0.5%) reduces carbon diffusion towards reverted austenite islands, thus further limiting stabilization of reverted austenite and lowering kinetics for martensite recovery. Molybdenum is effective in decreasing the diffusion coefficient of elements such as carbon and sulfur within ferritic/martensitic structures, because of its strong affinity for those elements [20,21]. Loveless et al. [22] worked with 13Cr4Ni alloys, finding that variants containing molybdenum presented increasing difficulties for hardness reduction through tempering.

Additionally, it was observed that the retained austenite in these alloys was rather unstable. As demonstrated by the results reported in Figure 14, there is an apparent destabilization effect of sub-zero cooling for Heat B. This aspect is believed to be important for mechanical components that work at low service temperatures and/or under manufacturing and service strains, since a loss in toughness and in corrosion resistance may be envisaged.

Under these circumstances, limiting the formation of reversed austenite is believed to be useful during tempering, and can be accomplished by increasing the Ac_1 critical temperature of the alloy as much as possible. This consequently allows for the recovery of the as-quenched microstructure at higher temperatures without the detrimental effect of austenite destabilization and the formation of virgin martensite upon cooling.

For example, Heats A and B appear different for experimental Ac_1 and Ms temperatures, with both temperatures being higher for Heat A (Ac_1 = 620 °C, Ms = 270 °C) than for Heat B (Ac_1 = 600 °C, Ms = 250 °C). These differences might be the consequence of higher carbon and nitrogen contents for Alloy B, with nickel and manganese contents of alloys being almost identical (Table 1). Therefore, more stringent control of carbon and nitrogen may be the key to controlling the final hardness of 13Cr-4Ni-(Mo) industrial heats.

A first attempt to verify these conclusions has been done with Heat C, reported in Table 4.

Table 4. Chemical composition of the alloy C.

Heat	%C	%Si	%Mn	%P	%Cr	%Mo	%S	%Ni	N (ppm)	%Cr_{eq}/%Ni_{eq}
C	0.018	0.420	0.68	0.023	12.53	0.53	0.001	4.00	68	2.70

The carbon content was reduced to 0.018% C, and the nitrogen content was reduced to 68 ppm. The predicted Ac_1 temperature for Heat C is 670 °C, which is about 15 °C higher than Heat A. From this it would be possible to increase tempering temperature without the formation of large volume fractions of unstable reverted austenite. Heat C was treated through double tempering at 665 and 615 °C. The final mechanical properties—averaged from seven different samples—gave the following results: YS = 583 MPa, UTS = 751 MPa, with hardness of 21.4 HRC. These results allow for the supposition that the reduction of both carbon level below 0.02% C and nitrogen below 100 ppm are effective in controlling the final hardness of 13Cr-4Ni-(Mo) with industrial heats below NACE recommendations (23 HRC), without an unacceptable loss of mechanical strength.

5. Conclusions

Control of the final mechanical properties of industrial 13Cr-4Ni-(Mo) heats has proven to be difficult when using double tempering treatments in accordance with NACE specifications.

From the results obtained here, this difficulty is mainly related to the quantity of austenite reversion that can form during tempering that—if it is not sufficiently stable—transforms into virgin martensite during cooling, thus limiting the effect of the tempering process.

This, in turn, is due to the relatively low Ac_1 temperatures of industrial heats, with the associated formation of unstable reverted austenite at temperatures above 600 °C.

Therefore, limiting the amount of austenite reversion is believed to be necessary while favoring the recovery of untempered martensite at tempering temperatures as high as possible, without allowing the formation of virgin martensite upon final cooling. Reduced carbon (<0.02% C) and nitrogen (<100 ppm) levels have proven effective in controlling the final hardness of 13Cr-4Ni-(Mo) industrial heats below NACE recommendations (23 HRC), without an unacceptable loss of mechanical strength.

Moreover, the retention of significant amounts of soft retained austenite at room temperature for 13Cr-4Ni-(Mo) alloys should be carefully considered, as this phase appeared to transform into martensite following a sub-zero treatment at −30 °C. This phenomenon could be detrimental for mechanical components working at low service temperatures and/or under service strains.

Nomenclature

Ac_1	Austenite transformation temperature
Cr_{eq}	Chromium equivalent (percentage of ferrite stabilizing elements)
δ, α', γ	phases designation
HB	Brinell hardness
HV	Vickers hardness
HR	Preliminary hot forging
HRC	Rockwell hardness, C scale
Ms	Martensite start temperature
Mf	martensite finish temperature
n	Instantaneous strain-hardening coefficient
Ni_{eq}	Nickel equivalent (weight percentage of austenite stabilizing elements)
OQ	Oil Quenched
UTS	Ultimate Tensile Strength
YS	Yield Strength

References

1. Kondo, K.; Ueda, M.; Ogawa, K.; Amaya, H.; Hirata, H.; Takabe, H.; Miyazaki, Y. Alloy design of super 13Cr martensitic stainless steel (Development of uper 13Cr martensitic stainless steel for line pipe-1). In Proceedings of the Supermartensitic Stainless Steels 99 Conference, Belgian, Brussels, 27–28 May 1999; pp. 11–18.

2. Niederau, H.J. A New Low-Carbon 16Cr-5Ni Stainless Martensitic Cast Steel. In *ASTM STP 756 Stainless Steel Castings*; Behal, V.G., Melilli, A.S., Eds.; American Society for Testing and Materials: West Conshohocken, PA, USA, 1982; pp. 382–393.

3. Nakada, N.; Tsuchiyama, T.; Takaki, S.; Miyano, N. Temperature Dependence of Austenite Nucleation Site on Reversion of Lath Martensite. *Mater. Sci. Forum* **2010**, *638–642*, 3424–3429. [CrossRef]

4. Liu, Z.B.; Yang, Z.Y.; Liang, J.X.; Zhang, L.N.; Zhang, X.L. Precipitation behavior and transformation kinetics of reverted austenite in ultra-high strength stainless steel. *Trans. Mater. Heat Treat.* **2010**, *31*, 39–44.

5. Park, E.S.; Yoo, D.K.; Sung, J.H.; Kang, C.Y.; Lee, J.H.; Sung, J.H. Formation of reversed austenite during tempering of 14Cr-7Ni-0.3Nb-0.7Mo-0.03C super martensitic stainless steel. *Met. Mater. Int.* **2004**, *10*, 521–525. [CrossRef]

6. De Sanctis, M.; Lovicu, G.; Valentini, R.; Dimatteo, A.; Ishak, R.; Migliaccio, U.; Montanari, R.; Pietrangeli, E. Microstructural Features Affecting Tempering Behavior of 16Cr-5Ni Supermartensitic Steel. *Metall. Mater. Trans. A* **2015**, *46*, 1878–1887. [CrossRef]

7. Song, Y.Y.; Li, X.Y.; Yin, F.X.; Ping, D.H.; Li, Y.Y. Variation of the Reversed Austenite Amount with the Tempering Temperature in a Fe-13%Cr-4%Ni-Mo Martensitic Stainless Steel. *Mater. Sci. Forum* **2010**, *650*, 193–198. [CrossRef]

8. Song, Y.Y.; Li, X.Y.; Rong, L.J.; Ping, D.H.; Yin, F.X.; Li, Y.Y. Formation of the reversed austenite during intercritical tempering in a Fe-13%Cr-4%Ni-Mo martensitic stainless steel. *Mater. Lett.* **2010**, *64*, 1411–1414. [CrossRef]

9. Bilmes, P.D.; Solari, M.; Llorente, C.L. Characteristics and effects of austenite resulting from tempering of 13Cr–NiMo martensitic steel weld metals. *Mater. Charact.* **2001**, *46*, 285–296. [CrossRef]

10. Lovicu, G.; De Sanctis, M.; Valentini, R.; Dimatteo, A.; Ishak, R.; Migliaccio, U.; Montanari, R.; Pietrangeli, E. Influence of presence and stability of reverted austenite on mechanical properties of 16Cr-5Ni supermartensitic stainless steel after tempering treatment. *Metall. Ital.* **2013**, *105*, 29–35.

11. Haynes, A.G. Some factors governing the metallurgy and voidability of 13%Cr and newer Cr-Ni martensitic stainless steels. In Proceedings of the Supermartensitic Stainless Steels '99, Brussels, Belgium, 27–28 May 1999.

12. Gooch, T.G. Heat treatment of welded 13% Cr-4% Ni martensitic stainless steels for sour service. *Weld. J.* **1995**, *74*, 213s–223s.

13. *APN005 Gleeble System Application Note*; Dynamic System Inc.: Poestenkill, NY, USA, 2001.

14. Colla, V.; De Sanctis, M.; Dimatteo, A.; Lovicu, G.; Valentini, R. Prediction of Continuous Cooling Transformation Diagrams for Dual-Phase Steels from the Intercritical Region. *Metall. Mater. Trans. A* **2011**, *42*, 2781–2793. [CrossRef]

15. American Society for Testing and Materials. *ASTM E975 Standard Practice for X-ray Determination of Retained Austenite in Steel with Near Random Cryslalographic Orientation*; ASTM: Philadelphia, PA, USA, 2003.

16. De Moor, E.; Föjer, C.; Clarke, A.J.; Penning, J.; Speer, J.G. Quench & partitioning response of a Mo-alloyed CMnSi steel. In Proceedings of the New Developments on Metallurgy and Applications of High Strength Steels Conference, Buenos Aires, Argentina, 26–28 May 2008; The Minerals, Metals & Materials Society: Warrendale, PA, USA, 2008; pp. 721–729.

17. Fisher, R.B.; Larson, J.A. Experience and some pitfalls in processing CA6NM. In Proceedings of the Transactions of the American Foundrymen's Society, AFS Annual Meeting, Chicago, IL, USA, 19–23 April 1982; pp. 103–113.

18. Sherman, E.T.; Nalbone, C.S.; Scott, W.D. Processing low-carbon CA6NM (steel) to meet NACE (National Association of Corrosion Engineers) hardness requirements. In Proceedings of the 28th Annual Conference, Technical Advances in Steel Castings, Coventry, UK, 24–25 May 1983; Steel Castings Research and Trade Associations: Sheffield, UK, 1983.

19. Gooch, T.G.; Woollin, P.; Haynes, A.G. Welding Metallurgy of Low Carbon 13% Chromium Martensitic Steels. In Proceedings of the Supermartensitic Stainless Steels '99, Brussels, Belgium, 27–28 May 1999; pp. 188–195.

20. Wada, H.; Pehlke, R.D. Nitrogen solubility and nitride formation in austenitic Fe-Ti alloys. *Metall. Trans. B* **1985**, *16*, 815–822. [CrossRef]

21. Akben, M.G.; Bacroix, B.; Jonas, J.J. Effect of vanadium and molybdenum addition on high temperature recovery, recrystallization and precipitation behavior of niobium-based microalloyed steels. *Acta Metall.* **1983**, *31*, 161–174. [CrossRef]

22. Loveless, R.W.; Smith, W.C.; Templeton, N.C. *Mechanical Testing for Deformation Model Development, ASTM STP 765*; ASTM: Philadephia, PA, USA, 1982; pp. 394–402.